Journal of
Applied Crystallography
ISSN 0021-8898
Editor: **Anke R. Kaysser-Pyzalla**

Single-crystal CVD diamonds as small-angle X-ray scattering windows for high-pressure research

Suntao Wang, Yu-fei Meng, Nozomi Ando, Mark Tate, Szczesny Krasnicki, Chih-shiue Yan, Qi Liang, Joseph Lai, Ho-kwang Mao, Sol M. Gruner and Russell J. Hemley

J. Appl. Cryst. (2012). **45**, 453–457

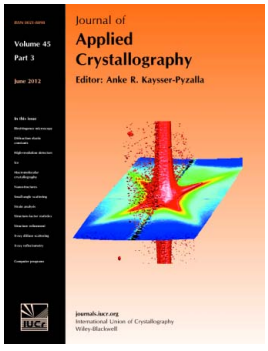

Journal of
Applied Crystallography
ISSN 0021-8898

Received 21 October 2011
Accepted 11 March 2012

Single-crystal CVD diamonds as small-angle X-ray scattering windows for high-pressure research

Suntao Wang,[a,b] Yu-fei Meng,[c] Nozomi Ando,[d] Mark Tate,[a] Szczesny Krasnicki,[c] Chih-shiue Yan,[c] Qi Liang,[c] Joseph Lai,[c] Ho-kwang Mao,[c] Sol M. Gruner[a,b]* and Russell J. Hemley[c]*

[a]Laboratory of Atomic and Solid State Physics, Cornell University, Ithaca, NY 14853, USA, [b]Cornell High Energy Synchrotron Source (CHESS), Cornell University, Ithaca, NY 14853, USA, [c]Geophysical Laboratory, Carnegie Institution of Washington, Washington, DC 20015, USA, and [d]Department of Chemistry, Massachusetts Institute of Technology, Cambridge, MA 02139, USA. Correspondence e-mail: smg26@cornell.edu, rhemley@ciw.edu

Small-angle X-ray scattering (SAXS) was performed on single-crystal chemical vapor deposition (CVD) diamonds with low nitrogen concentrations, which were fabricated by microwave plasma-assisted chemical vapor deposition at high growth rates. High optical quality undoped 500 µm-thick single-crystal CVD diamonds grown without intentional nitrogen addition proved to be excellent as windows on SAXS cells, yielding parasitic scattering no more intense than a 7.5 µm-thick Kapton film. A single-crystal CVD diamond window was successfully used in a high-pressure SAXS cell.

1. Introduction

Small-angle X-ray scattering (SAXS) is a powerful method for analyzing the structure of materials. The technique yields global information, such as particle sizes and size distributions from 1 to 100 nm, and shape and orientation distributions, in liquids, powders and bulk samples. This technique is becoming increasingly important and is often combined with electron microscopy to determine nanoscale structures. Applications range across the materials and life sciences. Recent specific examples include SAXS characterization of hydrogen storage materials, solid oxide fuel cells, chalcogenide glasses, aluminas, microemulsions, nucleic acids, proteins, mesoporous materials, inorganic polymers, coal samples, precipitation processes in the production of value-added zirconia, iron overload research in mammalian tissues *etc.*

In most SAXS applications the samples are enclosed in a sample cell with X-ray windows. The windows may be important not only for containing the samples but also to fix the path length, as in spectroscopic studies. A good SAXS window must satisfy several requirements. The window material must be transparent to X-rays and exhibit very little small-angle scattering compared with the sample of interest. The window scattering should be symmetrical about the beam center in applications where azimuthal integration is required. An ideal SAXS window must also show uniform scattering that is insensitive to slight changes in the cell position due to sample removal and loading. Finally, the window must be chemically inert to the samples it contains. Typical SAXS windows are made of low-Z materials such as diamond or beryllium, or very thin layers of Kapton, Mylar, polycarbonate or mica. High-pressure SAXS is especially taxing because the windows not only must be capable of withstanding high pressures with acceptable deformation, but also tend to be thick, which increases the background window scattering. Both beryllium and diamond windows have been used for this application in the past, but diamonds are more convenient for their optical transparency and safety (Ando, Chenevier *et al.*, 2008) and have multiple superlative properties, including the highest known hardness, very low friction and adhesion, unmatched thermal conductivity, good electronic mobility, a high melting temperature, the highest electron dispersion, high dielectric breakdown strength, radiation hardness, biocompatibility and unique chemical inertness (Asmussen & Reinhard, 2002). While a limited number of SAXS studies have been reported on synthetic and natural diamonds, it has been shown that nitrogen-free diamonds and diamonds with a low degree of aggregation yield little parasitic scattering (Shiryaev *et al.*, 2000, 2001, 2003; Shiryaev & Boesecke, 2011). However, these diamonds with low nitrogen contents, classified as type IIa diamonds, are very rare in nature and only make up 1–2% of all natural diamonds; 98% of natural diamonds are type I diamonds containing significant quantities of nitrogen, in the region of 100–1000 parts per million (Field, 1992).

Recent developments in microwave plasma-assisted chemical vapor deposition (MPCVD) diamond synthesis have enabled unprecedented growth rates of single-crystal diamonds (McCauley & Vohra, 1995; Yan *et al.*, 2002; Williams & Jackman, 2004; Mokuno *et al.*, 2005; Tallaire *et al.*, 2005; Sternschulte *et al.*, 2006; Yamada *et al.*, 2007) of high optical quality (Meng *et al.*, 2012), changing the prospects for the application of single-crystal CVD diamonds as window materials for SAXS. With MPCVD techniques, single-crystal diamonds can be produced to multicarat sizes at very high

growth rates (~200 μm h^{-1}) (Yan *et al.*, 2002). Single crystals above 12 mm thickness (or 10 carats in size) having a variety of optical and mechanical properties have been synthesized (Yan *et al.*, 2002, 2004; Hemley *et al.*, 2005; Ho *et al.*, 2006; Meng *et al.*, 2008; Liang *et al.*, 2009). High-quality optical components have been fabricated from undoped single-crystal MPCVD diamond materials, either as flat plate windows or as three-dimensional shapes such as anvils, with large dimensions that are not easily possible with natural diamonds (Meng *et al.*, 2012). These type IIa single-crystal MPCVD diamonds have been shown to sustain the generation of multimegabar pressures (1 bar = 100 000 Pa) (Mao *et al.*, 2003). In addition, MPCVD methods have been used to repair and augment natural diamond anvils, allowing containment of hydrogen to megabar pressures (Zha *et al.*, 2009). While in the past CVD diamonds have been largely disregarded as SAXS windows (Henderson, 1995), technical advancement in MPCVD synthesis prompts renewed interest in these materials. In this paper, synchrotron SAXS studies were performed to demonstrate that high optical quality single-crystal MPCVD diamonds with low nitrogen content are excellent materials for SAXS windows.

2. Experimental methods

All the CVD diamonds examined in this study were MPCVD single-crystal diamonds. They were produced in a microwave plasma CVD system using high power density (50–100 W cm^{-3}) microwave discharges operating at pressures of 100–200 Torr (1 Torr = 133.322 Pa) and temperatures of 1273–1773 K with gas mixtures of 10–20% CH_4/H_2. Deposition rates were typically 50–100 μm h^{-1} (Yan *et al.*, 2002, 2004; Ho *et al.*, 2006; Meng *et al.*, 2008; Liang *et al.*, 2009). The as-grown single-crystal CVD diamonds were laser cut into discs of 3.0 mm diameter and polished on both sides to a final thickness of 0.5 mm (Fig. 1*a*).

The nitrogen content and optical quality of the single-crystal CVD diamonds were characterized by micro-photoluminescence, and by UV–Vis and IR absorption spectroscopy. Micro-photoluminescence (PL) and Raman measurements were performed using a confocal micro-optical system with fiber optics and a solid-state laser of 457 nm operated at 50 mW at room temperature. UV–Vis absorption spectra were measured at room temperature using a Shimadzu UV–Vis scanning spectrophotometer. IR absorption spectra were acquired using a Varian 670-IR Fourier transform IR spectrometer in the range 400–12000 cm^{-1}.

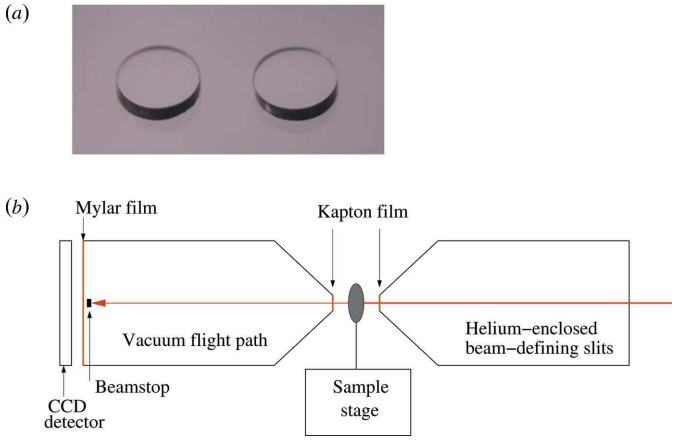

Figure 1
(*a*) Single-crystal CVD diamond windows for SAXS, 3.0 mm in diameter and 0.5 mm thick. (*b*) A simplified diagram of the SAXS beamline layout. The three windows along the X-ray beam path are two 12 μm-thick Kapton films and one 50 μm-thick Mylar film.

Synchrotron SAXS measurements were performed at the CHESS G1 Station. The X-ray beams had fluxes of 10^{10}–10^{12} photons per second at energies of 9.5–12 keV. Exposure times were 1–4 s. Fig. 1(*b*) shows the SAXS beamline setup. Upstream of the sample, the beam was defined by helium-enclosed slits to a size of 0.25 × 0.25 mm or 0.10 × 0.10 mm, with a sufficiently low level of low-angle parasitic scattering to resolve diffraction from structures greater than 100 nm. To characterize the parasitic scattering, the window materials were mounted in air, with their faces normal to the beam, on an *X*–*Z* translation stage. A 1.25 m-long vacuum flight path was installed downstream of the sample. A pin-diode beam-stop blocked the direct beam close to the detector while recording the transmitted intensity, which was later used for normalizing the scattering profiles. The acquired SAXS images were integrated azimuthally about the beam center to produce one-dimensional profiles. In order to evaluate the radius of gyration (R_g) of the scatterers using the *GNOM* program (Svergun, 1992), the scattering profiles were normalized and then a background profile was subtracted, which is the scattering profile from either air or an undoped single-crystal CVD diamond. Guinier analysis was also applied in the low-q region of the SAXS profiles to estimate R_g [$q = (4\pi/\lambda)\sin\theta$, where θ is half the scattering angle and λ is the wavelength of the incident radiation].

X-ray topography experiments were carried out at the CHESS A2 Station. The X-ray beam size was broadened by two Si(531) crystals with the X-ray energy set to 11.94 keV. The effective X-ray beam size on the sample was 4 × 6 mm (vertical × horizontal). The area detector was a home-made lens-coupled CCD camera, which contains a gadolinium gallium garnet (GGG) single crystal, the top 10.5 μm of which is Eu doped so as to luminesce when exposed to X-rays. The luminescent layer is imaged with a lens system (NAVITAR zoom 6000) with a maximum resolution of ~10 μm but with a narrow field of view (2.5 mm). For large diamonds (>2.5 mm), the camera was translated horizontally and vertically to obtain their overall topography. Because all the diamond windows were cut in such a way that the [001] direction was roughly along the surface normal, the reflection geometry was used to record the {004} projection topography images.

3. Results and discussion

The SAXS from an ideal window (or system parasitic scattering) should be less than the scattering from the sample being studied. This requirement is particularly stringent in protein solution SAXS, where weak scattering from dilute

protein solutions must be accurately measured. In a typical SAXS beamline such as the CHESS G1 station (Fig. 1*b*), vacuum or helium-flushed flight paths are installed to minimize the background (air scattering). The three windows in the flight path that the X-ray beam passes through sequentially are two 12 µm-thick Kapton films and one 50 µm-thick Mylar film, which can hold a reasonably high vacuum (∼5 mTorr) and produce very low background scattering. As shown in Fig. 2(*b*), the scattering profile from the direct beam without any sample was the system parasitic scattering, which includes the scattering from the three windows as well as gas scattering along the flight path. When a single 7.5 µm-thick Kapton film was inserted on the sample stage, it yielded very little scattering (Fig. 2*b*). This is why thin Kapton films are typically used in protein solution SAXS (Ando, Chenevier *et al.*, 2008). However, an undoped 500 µm-thick single-crystal CVD diamond grown in the atmosphere without intentional nitrogen addition had a SAXS signal comparable to the background scattering of the direct beam, and showed scattering even less than or comparable to a single 7.5 µm-thick Kapton film, demonstrating that undoped single-crystal CVD diamonds are excellent window materials for SAXS.

By comparison, the type Ia natural diamonds examined here display more intense and/or anisotropic scattering, as previously observed (Woods, 1970; Shiryaev, 2007; Shiryaev & Boesecke, 2011). In one case, intense and isotropic scattering was observed (Figs. 3*a* and 3*b*). To evaluate the average R_g of the scatterers in this natural diamond, the profile of an undoped CVD diamond (Fig. 2*b*) was subtracted from the profile of the natural diamond. A pair distribution function (inset in Fig. 3*c*) was calculated from the background-subtracted profile in the range ∼0.01–0.2 Å^{-1} by the indirect Fourier transform method implemented in *GNOM* with a maximum size of 360 Å. The R_g determined from the pair distribution function was 121 Å, consistent with the value obtained by Guinier analysis of 128 Å and within the typical range for type Ia diamonds (Shiryaev *et al.*, 2003). Strong cross-shaped scattering was observed for another natural diamond, which had been used in a previously reported high-pressure SAXS cell (Ando, Chenevier *et al.*, 2008) (Fig. 3*d*). Such strongly anisotropic scattering is problematic for protein solution SAXS where scattering images are integrated azimuthally about the beam center. The undoped single-crystal CVD diamonds presented here show no anisotropy in the scattering and are thus promising materials as SAXS windows.

For further correlation between nitrogen content and X-ray scattering, various single-crystal CVD diamonds were examined by UV–Vis and IR absorption spectroscopy. Single-crystal CVD diamonds that displayed little parasitic scattering did not exhibit characteristic absorption bands in the one-phonon region (1000–1500 cm^{-1}) of the IR absorption spectrum associated with nitrogen impurities (Fig. 4*a*), showing that they are type IIa diamonds. These single-crystal CVD diamonds also had high transparency in the UV–Vis range (Fig. 4*b*) compared with typical nitrogen-containing diamonds (Liang *et al.*, 2009). The spectrum in Fig. 4(*b*) was not corrected for reflection.

Raman and PL measurements made on ten single-crystal CVD diamonds with low concentrations of nitrogen were correlated with SAXS intensities. As shown in Fig. 4(*c*), the single-crystal CVD diamond with the strongest parasitic scattering exhibited the highest PL intensities at 504 and 575 nm, which can be attributed to the presence of H3 (a pair of substitutional nitrogen atoms separated by a vacancy) (Zaitsev, 2001) and NV^0 (nitrogen-vacancy) defect centers. The single-crystal CVD diamond with the least parasitic scattering displayed the lowest PL intensities.

Scanning SAXS experiments were performed on several of the single-crystal CVD diamonds. The results indicate that

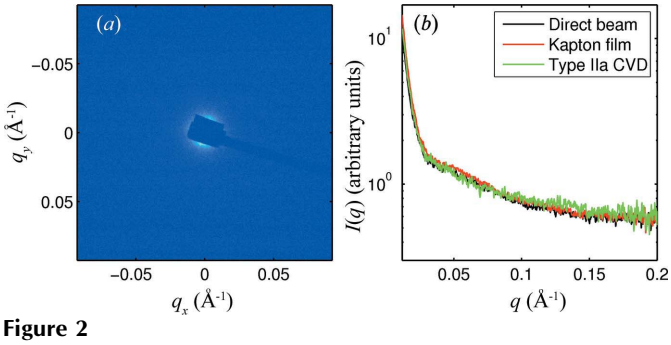

Figure 2
(*a*) SAXS image of an undoped single-crystal CVD diamond. (*b*) Scattering profiles from the air (black), a 7.5 µm-thick Kapton film (red) and an undoped single-crystal CVD diamond (green).

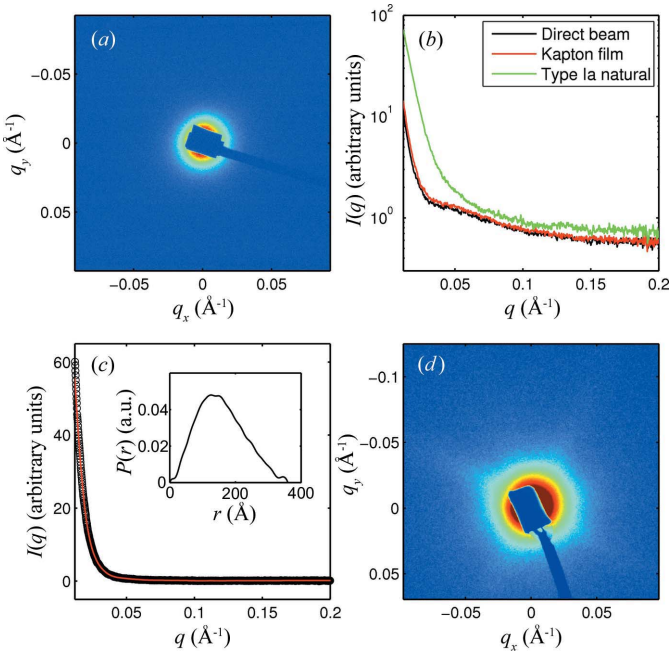

Figure 3
(*a*) SAXS image of a type Ia natural diamond displaying strong but isotropic scattering and (*b*) its scattering profile (green) compared with those of air (black) and a 7.5 µm-thick Kapton film (red). (*c*) The scattering profile from the type Ia natural diamond in (*a*) after background subtraction (black circles) and the *GNOM* fit (red line). Inset: pair distribution function obtained from *GNOM*. (*d*) SAXS image of another natural diamond, displaying strongly anisotropic cross-shaped scattering.

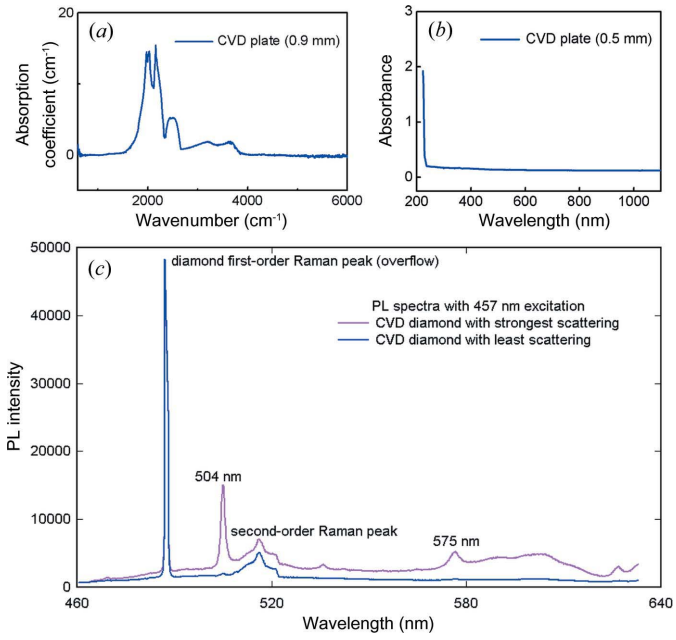

Figure 4
(*a*) IR and (*b*) UV–Vis absorption spectra of undoped single-crystal CVD diamond plates. (*c*) PL spectra of single-crystal CVD diamonds producing the strongest or least parasitic SAXS.

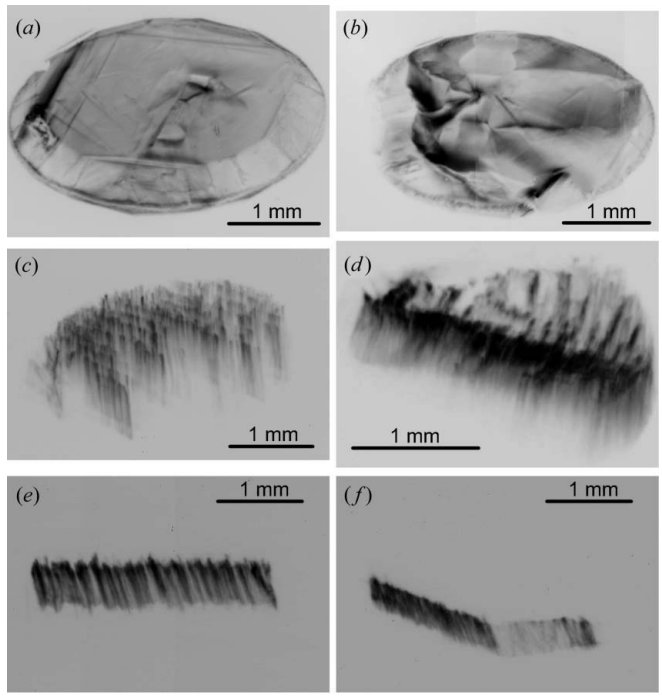

Figure 5
{004} projections of the topography of natural and single-crystal CVD diamonds. (*a*) A natural diamond that displays little parasitic scattering. (*b*) The type Ia natural diamond (the same as in Figs. 3*a*, 3*b* and 3*c*) that displays strong scattering. (*c*)–(*e*) Undoped single-crystal CVD diamonds that display almost no parasitic scattering; the diamond in (*d*) is the same as that in Fig. 2. (*f*) The single-crystal CVD diamond that displays strong scattering (Fig. 4*c*).

undoped single-crystal CVD diamonds show uniform and less scattering across different regions, while nitrogen-rich single-crystal CVD diamonds have more variation in scattering at different locations. X-ray topography was performed on both single-crystal CVD diamonds and natural diamonds in order to understand the origin of the strong SAXS. As shown in Fig. 5, natural diamonds exhibit a very different topography from single-crystal CVD diamonds. Line defects such as dislocations and planar defects such as stacking faults can be observed in natural diamonds (Figs. 5*a* and 5*b*), while dislocations are dominant in single-crystal CVD diamonds (Figs. 5*c* and 5*d*). These dislocations have line directions close to the [001] growth direction of single-crystal CVD diamonds, as previously observed by Gaukroger *et al.* (2008). In several single-crystal CVD diamonds, viewing only part or one section of the diamond when rocking the diffraction angle suggests that the diamond lattice planes are bent (Figs. 5*e* and 5*f*; see also the supporting videos available as supplementary materials[1]), an effect that originates from the specific growth parameters used (D. Popov *et al.*, manuscript in preparation). However, this bending nature is not responsible for the strong SAXS scattering, since single-crystal CVD diamonds producing no or strong parasitic scattering may both have bent planes (Figs. 5*e* and 5*f*).

Comparison of the scanning SAXS data and the topography shows that nitrogen-rich regions with variable scattering have similar topographies. In addition, undoped single-crystal CVD diamonds (Fig. 5*d*) showing negligible scattering also contain many line defects (dislocations). These results suggest that the line defects revealed by topography do not cause strong scattering in the typical q ranges for SAXS. The correlation between the scattering and PL data suggests that the increased incorporation of smaller-scale defect clusters (vacancy clusters, and clusters composed of both nitrogen and vacancy) may be the cause of the strong SAXS signal in single-crystal CVD diamonds, and these clusters are associated with higher growth rates catalyzed by the presence of nitrogen.

The performance of single-crystal CVD diamonds as window materials for protein solution SAXS was examined by a high-pressure protein unfolding study. An undoped single-crystal CVD diamond window (Figs. 2*a* and 5*d*) was used to replace a strongly scattering natural diamond (Fig. 3*d*) in a previously reported high-pressure SAXS cell (Ando, Chenevier *et al.*, 2008). The destabilized L99A mutant of T4 lysozyme was characterized up to 300 MPa, as previously described by Ando, Barstow *et al.* (2008). No pressure dependence was observed for the window scattering (Fig. 6*a*), enabling unambiguous background subtraction (Fig. 6*b*) and subsequent Guinier analysis (Fig. 6*b*, inset). Consistent with previous results (Ando, Barstow *et al.*, 2008), pressure-induced unfolding is observed with a pressure midpoint around 150 MPa and with a final R_g of ~30 Å. These results demonstrate that high-quality single-crystal CVD diamonds synthesized by MPCVD methods are excellent window materials for protein solution SAXS studies, while displaying superior

[1] Supplementary materials discussed in this paper are available from the IUCr electronic archives (Reference: CE5128). Services for accessing this material are described at the back of the journal.

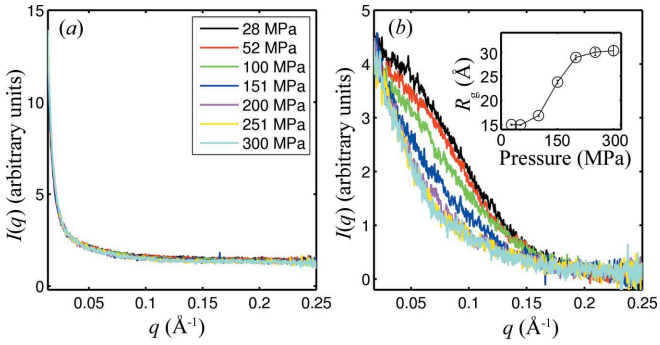

Figure 6
(*a*) Scattering profiles from buffers (50 m*M* glycine, 100 m*M* NaCl pH 3.0) at different pressures. (*b*) Buffer-subtracted scattering profiles of 10 mg ml^{-1} T4 lysozyme at 28, 52, 100, 151, 200, 251 and 300 MPa (from top to bottom). The inset shows the radius of gyration R_g of the protein as a function of pressure.

mechanical properties compared with typical window materials.

4. Conclusions

We have reported the first SAXS study of single-crystal CVD diamonds synthesized by MPCVD techniques. Parasitic scattering from single-crystal CVD diamonds was correlated with smaller-scale defect clusters detected by photoluminescence measurements, while larger-length-scale line defects observed by X-ray topography had no effect on the scattering or on the mechanical properties required for high-pressure studies. Our results demonstrate that even relatively thick undoped single-crystal CVD diamonds (500 µm) exhibit parasitic scattering less than or comparable to the thin Kapton films (7.5 µm) used for typical SAXS experiments. An undoped single-crystal CVD diamond proved to be an excellent window material in the characterization of protein unfolding at high pressures. These results suggest that the large high-quality single-crystal CVD diamonds achievable by modern MPCVD techniques may not only replace the typical SAXS windows currently in use but also enable new SAXS studies that would benefit from the large dimensions and structural rigidity of the windows.

The authors thank Y. F. Chen, L. Koerner and A. Woll for help with the high-pressure SAXS measurements, Y. Kim and J. Brock for help with the rocking-curve measurements, H. Shu and T. Yu for help with the polishing and growth of the CVD diamonds, and C. S. Zha and A. F. Goncharov for help with the Raman/PL and IR measurements. We are grateful to A. Kazmirov, A. Woll and K. Finkelstein for help with the synchrotron X-ray topography measurements. This work was supported by NSF-EAR, NSF-DMR, DOE-NNSA (CDAC), the Deborah Rose Foundation, the Balzan Foundation and DOE grant No. DEFG02-97ER62443. CHESS is supported by the NSF and NIH-NIGMS *via* NSF award No. DMR-0225180.

References

Ando, N., Barstow, B., Baase, W. A., Fields, A., Matthews, B. W. & Gruner, S. M. (2008). *Biochemistry*, **47**, 11097–11109.
Ando, N., Chenevier, P., Novak, M., Tate, M. W. & Gruner, S. M. (2008). *J. Appl. Cryst.* **41**, 167–175.
Asmussen, J. & Reinhard, D. (2002). Editors. *Diamond Films Handbook*. New York: Marcel Dekker.
Field, J. E. (1992). *The Properties of Natural and Synthetic Diamond*. London: Academic Press.
Gaukroger, M. P., Martineau, P. M., Crowder, M. J., Friel, I., Williams, S. D. & Twitchen, D. J. (2008). *Diamond Relat. Mater.* **17**, 262–269.
Hemley, R. J., Chen, Y. C. & Yan, C. S. (2005). *Elements*, **1**, 39–43.
Henderson, S. J. (1995). *J. Appl. Cryst.* **28**, 820–826.
Ho, S. S., Yan, C. S., Liu, Z., Mao, H. K. & Hemley, R. J. (2006). *Ind. Diamond Rev.* **66**, 28–32.
Liang, Q., Yan, C. S., Meng, Y., Lai, J., Krasnicki, S., Mao, H. K. & Hemley, R. J. (2009). *Diamond Relat. Mater.* **18**, 698–703.
Mao, W. L., Mao, H. K., Yan, C. S., Shu, J., Hu, J. & Hemley, R. J. (2003). *Appl. Phys. Lett.* **83**, 5190–5192.
McCauley, T. S. & Vohra, Y. K. (1995). *Appl. Phys. Lett.* **66**, 1486–1488.
Meng, Y. F., Yan, C. S., Krasnicki, S., Liang, Q., Lai, J., Shu, H., Yu, T., Steele, A., Mao, H. K. & Hemley, R. J. (2012). *Phys. Status Solidi A*, **209**, 101–104.
Meng, Y. F., Yan, C. S., Lai, J., Krasnicki, S., Shu, H., Yu, T., Liang, Q., Mao, H. K. & Hemley, R. J. (2008). *Proc. Natl Acad. Sci.* **105**, 17620–17625.
Mokuno, Y., Chayahara, A., Soda, Y., Horino, Y. & Fujimori, N. (2005). *Diamond Relat. Mater.* **14**, 1743–1746.
Shiryaev, A. A. (2007). *J. Appl. Cryst.* **40**, s116–s120.
Shiryaev, A. A. & Boesecke, P. (2011). http://arxiv.org/abs/1110.6270.
Shiryaev, A., Dembo, K., Klyuev, Yu., Naletov, A. & Feigelson, B. (2003). *J. Appl. Cryst.* **36**, 420–424.
Shiryaev, A. A., Hutchison, M. T., Dembo, K. A., Dembo, A. T., Iakoubovskii, K., Klyuev, Y. A. & Naletov, A. M. (2001). *Physica B*, **308–310**, 598–603.
Shiryaev, A. A., Klyuev, Y., Naletov, A., Dembo, K. & Feigelson, B. (2000). *Diamond Relat. Mater.* **9**, 1494–1499.
Sternschulte, H., Bauer, T., Schrenk, M. & Stritzker, B. (2006). *Diamond Relat. Mater.* **15**, 542–547.
Svergun, D. I. (1992). *J. Appl. Cryst.* **25**, 495–503.
Tallaire, A., Achard, J., Siliva, F., Sussmann, R. S. & Gicquel, A. (2005). *Diamond Relat. Mater.* **14**, 249–254.
Williams, O. A. & Jackman, R. (2004). *Diamond Relat. Mater.* **13**, 557–560.
Woods, G. S. (1970). *Philos. Mag.* **22**, 1081–1084.
Yamada, H., Chayahara, A., Mokuno, Y. & Shikata, S. I. (2007). *Diamond Relat. Mater.* **16**, 576–580.
Yan, C. S., Mao, H. K., Li, W., Qian, J., Zhao, Y. & Hemley, R. J. (2004). *Phys. Status Solidi A*, **201**, 25–27.
Yan, C. S., Vohra, Y. K., Mao, H. K. & Hemley, R. J. (2002). *Proc. Natl Acad. Sci.* **99**, 12523–12525.
Zaitsev, A. M. (2001). *Optical Properties of Diamonds*. Berlin: Springer-Verlag.
Zha, C. S., Krasnicki, S., Meng, Y. F., Yan, C. S., Lai, J., Liang, Q., Mao, H. K. & Hemley, R. J. (2009). *High Pressure Res.* **29**, 317–324.

Journal of Applied Crystallography

Volume 45, Part 3 (June 2012)

research papers

html pdf video buy

J. Appl. Cryst. (2012). **45** [doi:10.1107/S0021889812010722]

Single-crystal CVD diamonds as small-angle X-ray scattering windows for high-pressure research

S. Wang, Y. Meng, N. Ando, M. Tate, S. Krasnicki, C. Yan, Q. Liang, J. Lai, H. Mao, S. M. Gruner and R. J. Hemley

Abstract: Small-angle X-ray scattering (SAXS) was performed on single-crystal chemical vapor deposition (CVD) diamonds with low nitrogen concentrations, which were fabricated by microwave plasma-assisted chemical vapor deposition at high growth rates. High optical quality undoped 500 μm-thick single-crystal CVD diamonds grown without intentional nitrogen addition proved to be excellent as windows on SAXS cells, yielding parasitic scattering no more intense than a 7.5 μm-thick Kapton film. A single-crystal CVD diamond window was successfully used in a high-pressure SAXS cell.

Keywords: small-angle X-ray scattering; chemical vapor deposition; single-crystal diamonds; microwave plasma; high pressure.

play download

AVI file (10338.5 kbytes)
[doi:10.1107/S0021889812010722/ce5128sup1.avi]
A series of topography images at different diffraction angles from an undoped single-crystal CVD diamond displaying almost no parasitic scattering (the same one as in Figs. 2 and 5e).

play download

AVI file (16540.5 kbytes)
[doi:10.1107/S0021889812010722/ce5128sup2.avi]
A series of topography images at different diffraction angles from a single-crystal CVD diamond displaying strong parasitic scattering (the same one as in Figs. 4c and 5f).

Notes:

To open or display or play some files, you may need to set your browser up to use the appropriate software. See the full list of file types for an explanation of the different file types and their related mime types and, where available links to sites from where the appropriate software may be obtained.

The download button will force most browsers to prompt for a file name to store the data on your hard disk.

Where possible, images are represented by thumbnails.

download bibliographic record in BIBTeX format

Find reference: J. Appl. Cryst. **Volume** **Page** find

Search: **From** 1991 **to** 2012 search Advanced search